

Supplementary Figures

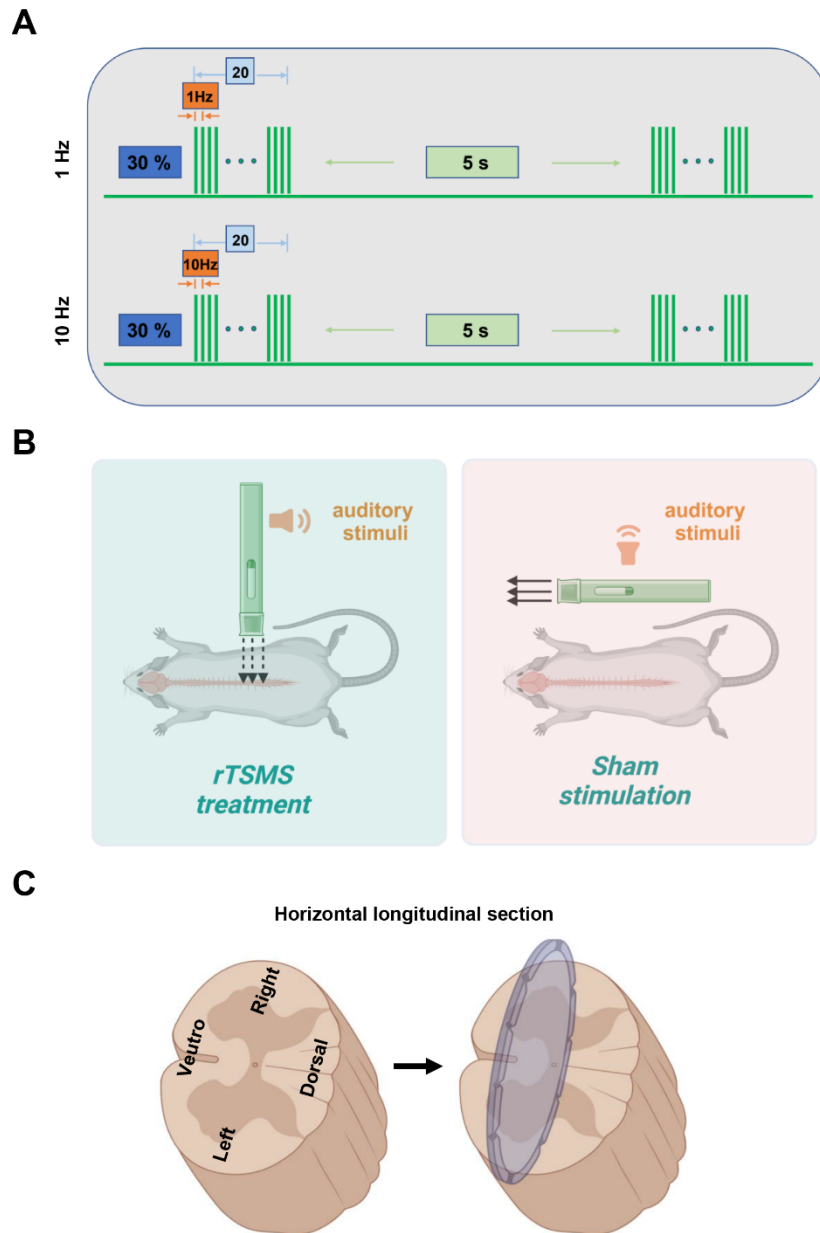


Figure S1. Low-frequency rTMS ameliorates lesion area and promotes neuronal survival in rats with SCI. (A) The 1Hz low-frequency rTMS and 10Hz high-frequency rTMS parameters. (B) The position of coil during rTMS treatment (left) and sham stimulation (right). Image was created with BioRender.com. (C) Schematic illustration of horizontal longitudinal section of the spinal cord. Image was created with BioRender.com.

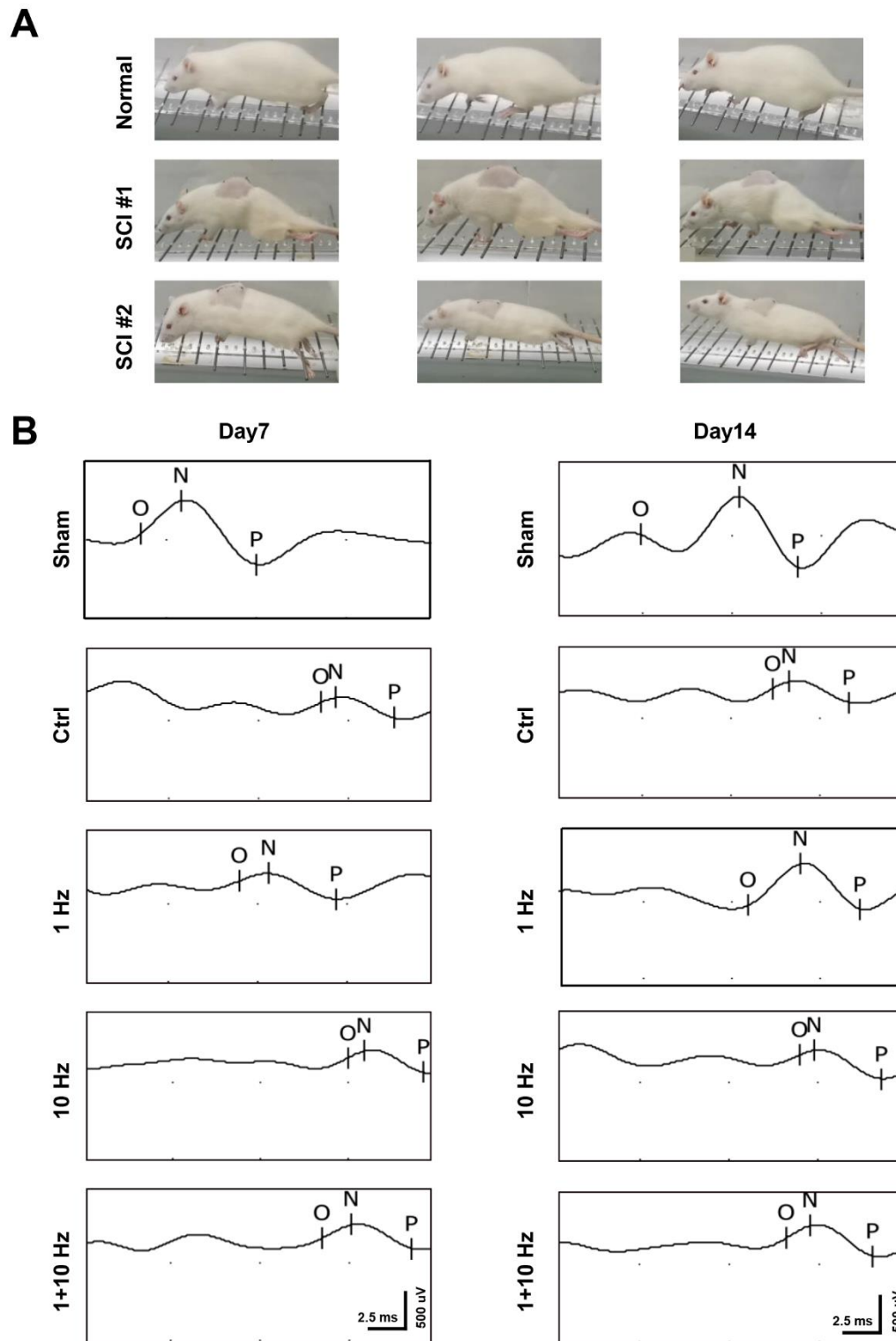


Figure S2. Low-frequency rTMS enhances motor and sensory function recovery following SCI. (A) Rats in the horizontal ladder test before and after SCI operation. (B) Representative individual electrophysiological traces at 7 and 14 dpi.

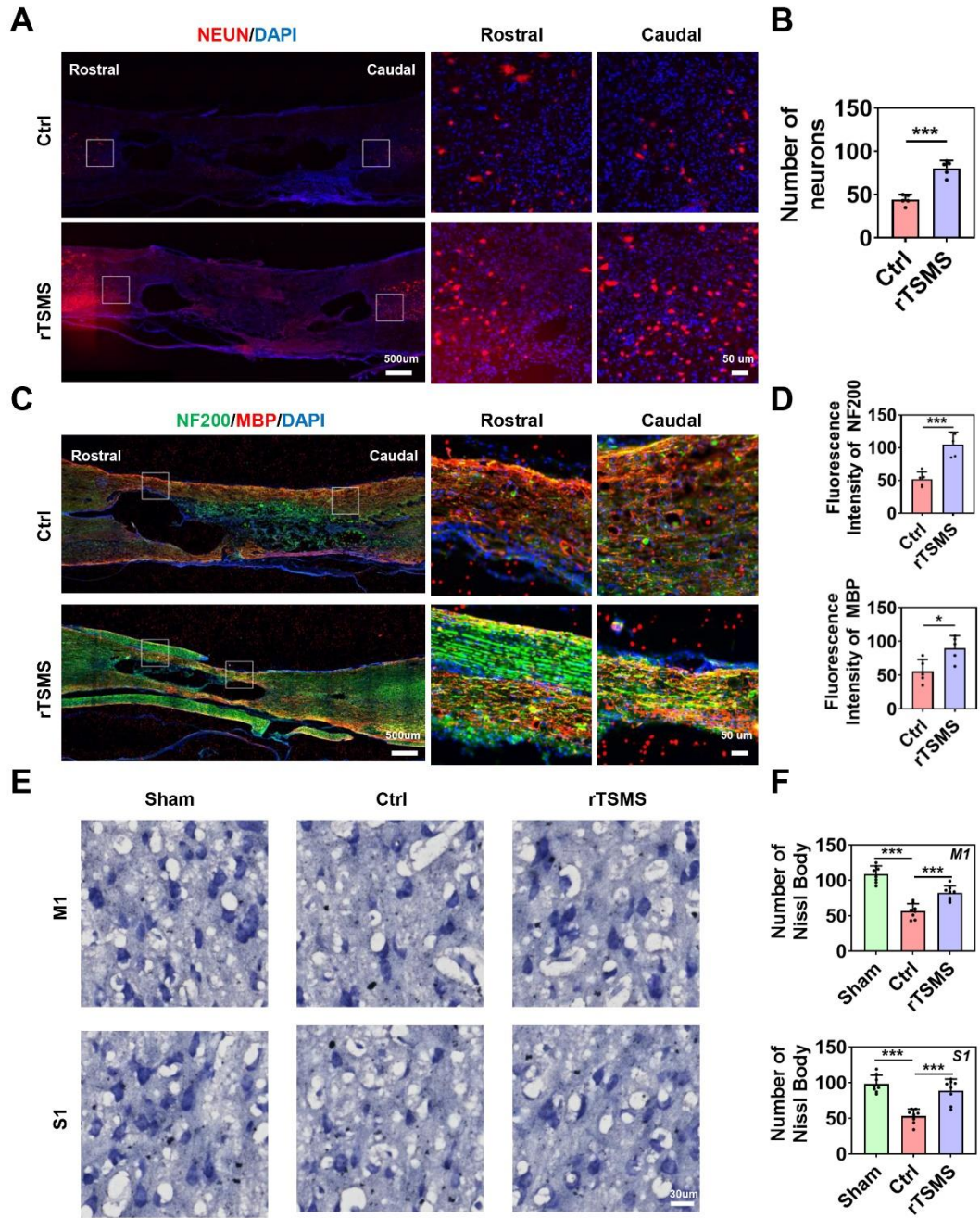


Figure S3. rTSMs enhances synapse formation and neuronal activity in rats with SCI. (A-B) Representative images of immunostaining and statistical analysis of NEUN (red) and DAPI (blue) in the injured spinal cord at 21 dpi, $n = 5$. (C-D) Representative images of immunostaining and statistical analysis of NF200 (green), MBP (red) and DAPI (blue) in the injured spinal cord at 21 dpi, $n = 5$. (E-F) Representative images and statistical analysis of Nissl body in the M1 and S1 regions at 21 dpi. $n = 8$. * $P < 0.05$, *** $P < 0.001$.

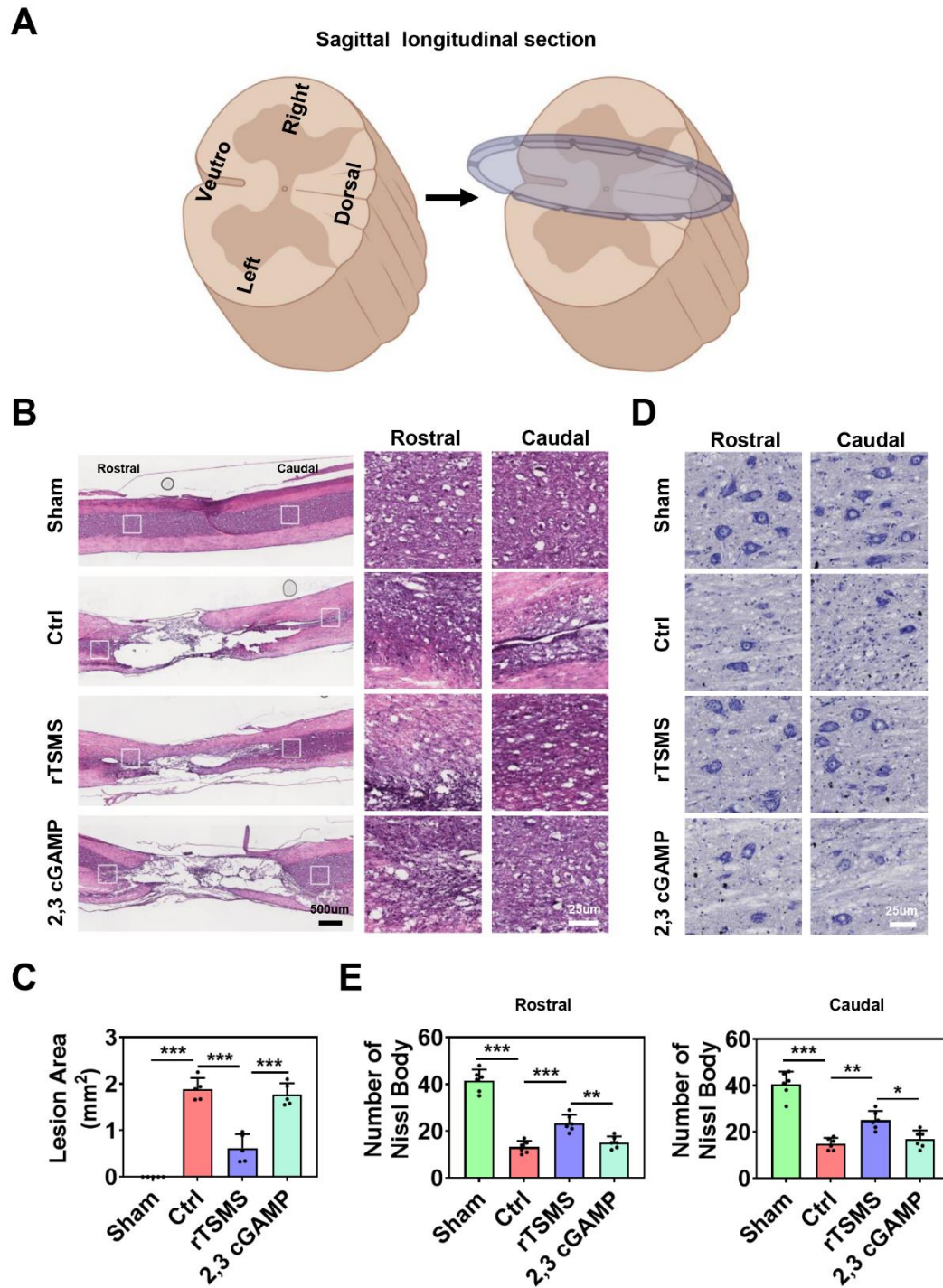


Figure S4. STING agonist diminishes the neuroprotective effects of rTSMS in SCI rats. (A) Schematic illustration of sagittal longitudinal section of the spinal cord. The image was created with BioRender.com. (B-C) Representative HE-stained images and quantification of the lesion area in rats at 21 dpi, $n = 5$. (D-E) Representative Nissl-stained images and quantification of Nissl body at 21 dpi, $n = 6$. * $P < 0.05$, ** $P < 0.01$, *** $P < 0.001$.